

SCATTERING PROCESSES IN THE MASSIVE SCHWINGER MODEL*

Christoph Adam[†]

*Center for Theoretical Physics
Laboratory for Nuclear Science
and Department of Physics
Massachusetts Institute of Technology
Cambridge, Massachusetts 02139
and
Inst. f. theoret. Physik d. Uni Wien
Boltzmannngasse 5, 1090 Wien, Austria*

(MIT-CTP-2602, hep-th/9701013. January 1997)

Abstract

We derive the (matrix-valued) Feynman rules of the mass perturbation theory and use it for the resummation of the n -point functions with the help of the Dyson-Schwinger equations. We use these results for a short review of the complete spectrum of the model and for a discussion of scattering processes. We find that in scattering cross sections all the resonances and higher particle production thresholds of the model are properly taken into account by our resummed mass perturbation theory, without the need of further approximations.

PACS-Numbers: 11.10, 11.80, 11.90

Typeset using REVTeX

[†]Email address: adam@ctp.mit.edu, adam@pap.univie.ac.at

*This work is supported by a Schrödinger Stipendium of the Austrian FWF and in part by funds provided by the U.S. Department of Energy (D.O.E.) under cooperative research agreement #DF-FC02-94ER40818.

I. INTRODUCTION

The massive Schwinger model is QED₂ with one massive fermion,

$$L = \bar{\Psi}(i\cancel{\partial} - e\cancel{A} + m)\Psi - \frac{1}{4}F_{\mu\nu}F^{\mu\nu} \quad (1)$$

Both massive and massless ($m = 0$) Schwinger model have been subject to intensive study as simple models that nevertheless show some nontrivial field theoretic features, like anomalies, nontrivial vacuum structure (θ vacuum), fermion condensates, etc. ([1] – [25]). Further, they have been used as test labors for the study of some concepts that are important for more realistic models like QCD (confinement, OPE, etc., [8], [26] – [30]).

The massless model may be solved exactly and is, in fact, equivalent to the theory of one free, massive boson (“Schwinger boson”) with mass $\mu_0^2 = \frac{e^2}{\pi}$ (here the nontrivial vacuum structure may be detected by chiral VEVs, leading e.g. to the fermion condensate).

In the massive model the Schwinger boson turns into an interacting particle with renormalized mass μ , that may form bound states and undergo scattering. Mass perturbation theory (which may be performed because of the exact solubility of the massless model) turns out to be especially useful for the discussion of these features, because it is formulated in terms of physical fields only (the Schwinger boson and chiral currents; the confined fermions themselves do not occur), and because the mass perturbation expansion is about the physical θ vacuum. Actually, the mass perturbation theory has some similarity with the chiral perturbation theory of QCD.

In this article we will systematically perform the mass perturbation expansion and derive the corresponding Feynman rules, which turn out to acquire a matrix structure because of the chiral properties of the model (i.e. because the mass term $m\bar{\Psi}\Psi$ mixes left- and right-handed fields). Further we will show how Schwinger boson n -point functions may be re-expressed in terms of chiral n -point functions by the use of the Dyson-Schwinger equations of the model. The latter ones may be resummed by further re-expressing them in terms of non-factorizable n -point functions. This resummation enables us to infer all the (stable) particle and (unstable) bound-state masses from the poles of the two-point function. We will find, as one result, that the spectrum of the model is richer than expected earlier ([17,32]). Further, by rewriting the higher n -point functions in terms of non-factorizable ones, we are able to identify all the possible final states of decays and scattering processes, and we may compute scattering cross sections that include the effects of all possible resonances and higher particle production thresholds.

All computations are based on the Euclidean path integral formalism, and therefore, we have to take care of our specific Euclidean conventions (see e.g. [12]) in the computations.

II. MASS PERTURBATION THEORY

First let us shortly review the mass perturbation theory. By simply expanding the mass term, the vacuum functional and VEVs of the massive model may be traced back to space-time integrations of VEVs of the massless model. E.g. the vacuum functional is

$$Z(m, \theta) = \sum_{k=-\infty}^{\infty} e^{ik\theta} N \int D\bar{\Psi}D\Psi DA_{\mu}^k.$$

$$\cdot \sum_{n=0}^{\infty} \frac{m^n}{n!} \prod_{i=1}^n \int dx_i \bar{\Psi}(x_i) \Psi(x_i) \exp \int dx \left[\bar{\Psi}(i\cancel{\partial} - e\cancel{A})\Psi - \frac{1}{4} F_{\mu\nu} F^{\mu\nu} \right] \quad (2)$$

(k ... instanton number). Therefore, one needs scalar VEVs $\langle S(x_1) \dots S(x_n) \rangle_0$ of the massless model, where $S = \bar{\Psi}\Psi$, $S_{\pm} = \frac{1}{2} \bar{\Psi}(1 \pm \gamma_5)\Psi$. Chiral VEVs $\langle S_{H_1} \dots S_{H_n} \rangle_0$, $H_i = \pm$, are especially easily computed, as only a definite instanton sector contributes (see e.g. [21,32,33]),

$$\langle S_{H_1}(x_1) \dots S_{H_n}(x_n) \rangle_0 = e^{ik\theta} \left(\frac{\Sigma}{2} \right)^n \exp \left[\sum_{i < j} (-)^{\sigma_i \sigma_j} 4\pi D_{\mu_0}(x_i - x_j) \right] \quad (3)$$

$$k = \sum_{i=1}^n \sigma_i = n_+ - n_-$$

where $\sigma_i = \pm 1$ for $H_i = \pm$, D_{μ_0} is the massive scalar propagator of the Schwinger boson ($\mu_0^2 = \frac{e^2}{\pi}$) and Σ is the fermion condensate of the massless model.

The Schwinger boson Φ is related to the vector current, $J_{\mu} = \frac{1}{\sqrt{\pi}} \epsilon_{\mu\nu} \partial^{\nu} \Phi$, and, therefore, the S and Φ VEVs, which we need for the perturbative calculation of massive VEVs, are related to the vector and scalar current VEVs of the massless model. Explicitly the S and Φ VEVs may be computed from the generating functional (which is at the same time a VEV for n chiral currents)

$$\langle S_{H_1}(x_1) \dots S_{H_n}(x_n) \rangle_0[\lambda] = e^{ik\theta} \left(\frac{\Sigma}{2} \right)^n \exp \left[\sum_{i < j} (-)^{\sigma_i \sigma_j} 4\pi D_{\mu_0}(x_i - x_j) \right] \cdot$$

$$\cdot \exp \left[- \int dy_1 dy_2 \lambda(y_1) D_{\mu_0}(y_1 - y_2) \lambda(y_2) + 2i\sqrt{\pi} \sum_{l=1}^n (-)^{\sigma_l} \int dy \lambda(y) D_{\mu_0}(y - x_l) \right] \quad (4)$$

(see [34] for an explicit computation), where λ is the external source for the Schwinger boson Φ . Observe the $(-)^{\sigma_l}$ in the last term of the exponent. As a consequence, whenever an *odd* number of external Φ lines meets at a point x_i , the corresponding $S_-(x_i)$ acquires a $-$, i.e. instead of a $S = S_+ + S_-$ vertex there is a $P = S_+ - S_-$ vertex.

From equs. (3), (4) one finds that exponentials $\exp \pm 4\pi D_{\mu_0}(x_i - x_j)$ are running from any vertex x_i to any other vertex x_j ; however, in order to get an IR finite perturbation theory, one has to expand these exponentials into the functions

$$E_{\pm}(x) = e^{\pm 4\pi D_{\mu_0}(x)} - 1, \quad (5)$$

(or their Fourier transforms $\tilde{E}_{\pm}(p)$ for momentum space Feynman rules). This expansion is analogous to the cluster expansion of statistical physics.

The important point is that each vertex contains (for $\theta \neq 0$) two types of vertices, $m \langle S(x) \rangle_0 = m(\langle S_+(x) \rangle_0 + \langle S_-(x) \rangle_0) \simeq m \frac{\Sigma}{2} e^{i\theta} + m \frac{\Sigma}{2} e^{-i\theta}$, and these two types of vertices are connected by two types of propagators, namely $S_+(x)S_+(y)$ and $S_-(x)S_-(y)$ by $E_+(x - y)$, and $S_+(x)S_-(y)$ and $S_-(x)S_+(y)$ by $E_-(x - y)$. Further, because all vertices may be connected to each other, up to $n - 1$ lines $E_{\pm}(x - y_i)$ may run from one vertex x to the other vertices y_i for a n -th order mass perturbation contribution.

As a consequence, the Feynman rules acquire a matrix structure. More precisely, the propagator corresponding to the $E_{\pm}(x)$ is a matrix, which in momentum space reads

$$\mathcal{E}(p) = \begin{pmatrix} \tilde{E}_+(p) & \tilde{E}_-(p) \\ \tilde{E}_-(p) & \tilde{E}_+(p) \end{pmatrix} \quad (6)$$

where the individual entries correspond to the individual $\langle S_i(x)S_j(y) \rangle_0$, $i, j = \pm$, propagators.

Each vertex, where n propagator lines $\mathcal{E}(p_i)$ meet, is a n -th rank tensor \mathcal{G} . Only two components of this tensor are nonzero, namely

$$\mathcal{G}_{++++} = g_{\theta} \quad , \quad \mathcal{G}_{----} = g_{\theta}^* \quad (7)$$

(corresponding to $S = S_+ + S_-$). E.g. the vertex where two propagators meet is a matrix

$$\mathcal{G} = \begin{pmatrix} g_{\theta} & 0 \\ 0 & g_{\theta}^* \end{pmatrix}. \quad (8)$$

where g_{θ}, g_{θ}^* are the renormalized couplings including all tadpole-like corrections (see e.g. [32]),

$$g_{\theta} = m \frac{\Sigma}{2} e^{i\theta} + o(m^2). \quad (9)$$

Internal lines must be $\mathcal{E}(p)$ because of the Feynman rules; external lines, however, may be boson lines, too, when we treat bosonic n -point functions $\langle \Phi(x_1) \dots \Phi(x_n) \rangle_m$. There the rule is that, when the external boson lines are amputated, the vertex where they meet is multiplied by P (S) when an odd (even) number of bosons meets at that vertex, where

$$P = \begin{pmatrix} 1 \\ -1 \end{pmatrix} \quad , \quad S = \begin{pmatrix} 1 \\ 1 \end{pmatrix}. \quad (10)$$

These Feynman rules may be given by the graphs of Fig. 1 (we display them in momentum space)

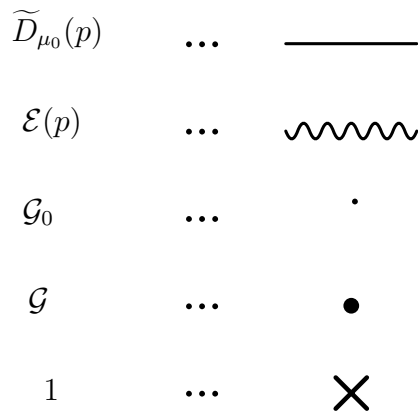


Fig. 1

where \mathcal{G}_0 denotes the bare coupling. Let us e.g. investigate the connected two-point function $\langle i\Phi(x_1)i\Phi(x_2) \rangle_m^c$ within mass perturbation theory. After amputation of the two

external boson lines, and ignoring the P vectors (10) at the initial and final vertices we find the following graphical representation (see Fig. 2a, b)

$$\text{---} \bigcirc \text{---} = \text{---} \text{---} + \text{---} \bigcirc \text{---}$$

Fig. 2a

$$\begin{aligned} \text{---} \bigcirc \text{---} &= \bullet + \text{---} \bullet + \text{---} \bullet \text{---} + \text{---} \bullet \text{---} \text{---} \bullet + \text{---} \bullet \text{---} \text{---} \bullet \text{---} \bullet + \\ &\text{---} \bullet \text{---} \text{---} \bullet \text{---} \bullet \text{---} \bullet + \text{---} \bullet \text{---} \text{---} \bullet \text{---} \bullet \text{---} \bullet + \text{---} \bullet \text{---} \text{---} \bullet \text{---} \bullet \text{---} \bullet + \dots \end{aligned}$$

Fig. 2b

where always the left and right vertices are the initial and final ones. Observe that we do not draw graphs where a sequence of wavy lines begins and ends at the same vertex, because they are already taken into account by the renormalized coupling \mathcal{G} .

Introducing for the above two-point function (Fig. 2b) the name $\mathcal{G}\Pi(p)$ in momentum space (matrix multiplication is understood)

$$\mathcal{G}\Pi(p) := \mathcal{G} + \mathcal{G}\mathcal{E}(p)\mathcal{G} + \mathcal{G}\mathcal{E}(p)\mathcal{G}\mathcal{E}(p)\mathcal{G} + \dots \quad (11)$$

we will find a resummation for $\Pi(p)$ that relies on the following observation. All diagrams that fall into two pieces when they are cut at a vertex, factorize in momentum space, i.e. they are a product of two functions of p . The opposite type graphs are called non-factorizable (n.f.).

Here we should be more precise about the cutting. We stated above that the vertices are tensors, so how to cut such a vertex? Suppose e.g. we have a vertex where three lines meet and we want to cut it in a way that two wavy lines belong to the left hand side, and one line to the right hand side. Then we rewrite the vertex like

$$\mathcal{G}_{ijk} = \delta_{ijl}\mathcal{G}_{l'k} \quad , \quad i, j, k, l, l' = \pm \quad (12)$$

where $\mathcal{G}_{ll'}$ is the vertex matrix (8) and the $\delta_{i_1\dots i_n}$ are generalizations of the Kronecker delta δ_{ij} , i.e.

$$\delta_{++++} = \delta_{-----} = 1 \quad , \quad \delta_{i_1\dots i_n} = 0 \quad \text{otherwise} \quad (13)$$

Therefore, we may write for the sum of non-factorizable graphs, which we call \mathcal{A} (see Fig. 3)

$$\text{---} \times \text{---} \times + \text{---} \times \text{---} \times + \text{---} \times \text{---} \times + \text{---} \times \text{---} \times + \dots$$

Fig. 3

$$\mathcal{A}_{ij}(p) = \mathcal{E}_{ij}(p) + \int \frac{d^2q}{(2\pi)^2} \delta_{ikk'} \mathcal{E}_{kl}(q) \mathcal{G}_{ll'} \mathcal{E}_{l'm}(q) \mathcal{E}_{k'm'}(q-p) \delta_{jmm'} + \dots \quad (14)$$

The matrix $\mathcal{A}(p)$ may be rewritten like

$$\mathcal{A}(p) = \begin{pmatrix} \langle \widetilde{S}_+ \widetilde{S}_+ \rangle_{\text{n.f.}}(p) & \langle \widetilde{S}_+ \widetilde{S}_- \rangle_{\text{n.f.}}(p) \\ \langle \widetilde{S}_- \widetilde{S}_+ \rangle_{\text{n.f.}}(p) & \langle \widetilde{S}_- \widetilde{S}_- \rangle_{\text{n.f.}}(p) \end{pmatrix} \quad (15)$$

The entries of this matrix are, however, related (e.g. $\langle \widetilde{S}_- \widetilde{S}_- \rangle_{\text{n.f.}}(g_\theta, p) = \langle \widetilde{S}_+ \widetilde{S}_+ \rangle_{\text{n.f.}}(g_\theta^*, p)$, as may be checked from the perturbative expansion) and, therefore, we find for the product $\mathcal{G}\mathcal{A}(p)$ (which we need in the sequel)

$$\mathcal{G}\mathcal{A}(p) =: \begin{pmatrix} \alpha(g_\theta, p) & \beta(g_\theta, p) \\ \beta(g_\theta^*, p) & \alpha(g_\theta^*, p) \end{pmatrix} \quad (16)$$

$$\alpha(g_\theta, p) = g_\theta \langle \widetilde{S}_+ \widetilde{S}_+ \rangle_{\text{n.f.}}(g_\theta, p) \quad , \quad \beta(g_\theta, p) = g_\theta \langle \widetilde{S}_+ \widetilde{S}_- \rangle_{\text{n.f.}}(g_\theta, p). \quad (17)$$

(Remark: in [32] we wrote $\alpha^*(g_\theta, p), \beta^*(g_\theta, p)$ instead of $\alpha(g_\theta^*, p), \beta(g_\theta^*, p)$. This makes no difference as long as the propagator functions $\widetilde{E}_\pm(p)$ themselves are purely real (or one needs the real part only). However, when the propagators acquire imaginary parts, equ. (16) is the correct one.)

Now we may collect all n.f. graphs in (11), Fig. 2b, e.g. on the left hand side, and find that they are again multiplied by *all* graphs that occur in Fig. 2b. Therefore we may write for $\mathcal{G}\Pi(p)$ of equ. (11)

$$\mathcal{G}\Pi(p) = \mathcal{G}(\mathbf{1} + \mathcal{A}(p)\mathcal{G}\Pi(p)). \quad (18)$$

Equation (18) may be solved for $\Pi(p)$ by a matrix inversion and has the solution

$$\Pi(p) = \frac{1}{N(p)} \begin{pmatrix} 1 - \alpha(g_\theta^*, p) & \beta(g_\theta^*, p) \\ \beta(g_\theta, p) & 1 - \alpha(g_\theta, p) \end{pmatrix} \quad (19)$$

where $N(p)$ is the determinant of the matrix that had to be inverted,

$$N(p) = \det(\mathbf{1} - \mathcal{G}\mathcal{A}(p)) = 1 - \alpha(g_\theta, p) - \alpha(g_\theta^*, p) + \alpha(g_\theta, p)\alpha(g_\theta^*, p) - \beta(g_\theta, p)\beta(g_\theta^*, p). \quad (20)$$

III. DYSON-SCHWINGER EQUATIONS AND HIGHER N -POINT FUNCTIONS

Observe that the relation (Fig. 2a) between the amputated Schwinger-boson two-point function and the graph (Fig. 2b) for $\mathcal{G}\Pi(p)$ is the first Dyson-Schwinger equation of the model that may be derived from the equation of motion

$$M_x i\Phi(x) := (\square_x - \mu_0^2) i\Phi(x) = 2\sqrt{\pi} m P(x). \quad (21)$$

Defining the Fourier transforms

$$M^{(n)}(p_1, \dots, p_n) := \text{FT}(M_{x_1} \dots M_{x_n} \langle i\Phi(x_1) \dots i\Phi(x_n) \rangle_m^c) \quad (22)$$

Fig. 2a may be written like ($M^{(2)}(p, p) \equiv M^{(2)}(p)$)

$$M^{(2)}(p) = -(p^2 + \mu_0^2) + 4\pi m\langle S \rangle_m + 4\pi m^2 \langle \widetilde{PP} \rangle_m^c(p) \quad (23)$$

where

$$m\langle S \rangle_m \equiv P^T \mathcal{G} P = S_i \mathcal{G}_i = g_\theta + g_\theta^* \quad (24)$$

$$m^2 \langle \widetilde{PP} \rangle_m^c(p) \equiv P^T \mathcal{G} (\Pi(p) - \mathbf{1}) P \quad (25)$$

where $P^T = (1, -1)$ is the transpose of the vector P , (10), and matrix multiplication is understood (the single vertex \mathcal{G} we may interpret either as a two-component object that is contracted by two vectors P or as a one-component object that is contracted by one vector S).

In Fig. 2a we did not display the 4π factors of (23), and we will continue not to display them in the figures (however, we, of course, retain them in the formulae).

Analogously one may find higher Dyson-Schwinger equations. Before showing them we need some more graphical rules (see Fig. 4)

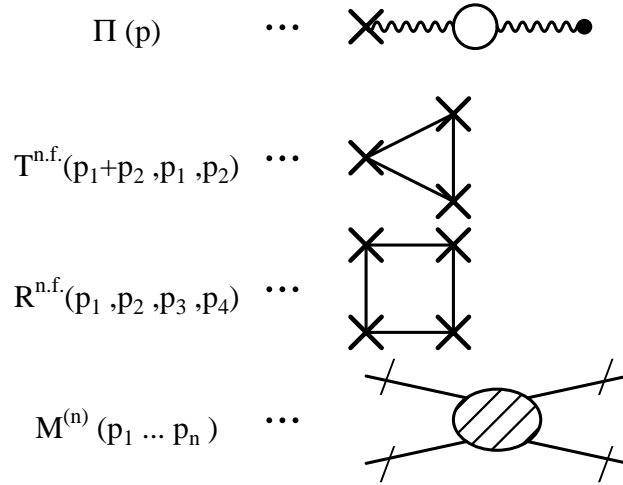


Fig. 4

where $M^{(n)}$, of course, should have n external (amputated) boson lines. For the three-point function e.g. we find the Dyson-Schwinger equation

$$\begin{aligned} M^{(3)}(p_1 + p_2, p_1, p_2) &= (2\sqrt{\pi})^3 [m\langle P \rangle_m + m^2 \langle \widetilde{SP} \rangle_m^c(p_1 + p_2) \\ &+ m^2 \langle \widetilde{SP} \rangle_m^c(p_1) + m^2 \langle \widetilde{SP} \rangle_m^c(p_2) + m^3 \langle \widetilde{PPP} \rangle_m^c(p_1 + p_2, p_1, p_2)] \end{aligned} \quad (26)$$

where $m\langle P \rangle_m$ and $m^2 \langle \widetilde{SP} \rangle_m^c(p)$ are analogous to (24), (25) whereas the last term is given by

$$m^3 \langle \widetilde{PPP} \rangle_m^c(p_1 + p_2, p_1, p_2) = P_i P_j P_k \mathcal{G}_{ii'} \mathcal{G}_{jj'} \mathcal{G}_{kk'} T_{i'j'k'}(p_1 + p_2, p_1, p_2) \quad (27)$$

and T_{ijk} is given by the graphs of Fig. 5

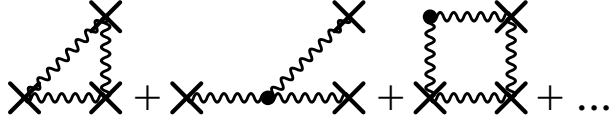


Fig. 5

The essential point is that $M^{(3)}$, again, may be reexpressed entirely in terms of non-factorizable n -point functions, namely

$$M^{(3)}(p_1 + p_2, p_1, p_2) = (2\sqrt{\pi})^3 P_i P_j P_k \Pi_{ii'}(p_1 + p_2) \Pi_{jj'}(p_1) \Pi_{kk'}(p_2) \cdot \left(\mathcal{G}_{i'j'k'} + \mathcal{G}_{i'l} \mathcal{G}_{j'm} \mathcal{G}_{k'n} T_{lmn}^{\text{n.f.}}(p_1 + p_2, p_1, p_2) \right) \quad (28)$$

or, graphically (see Fig. 6)

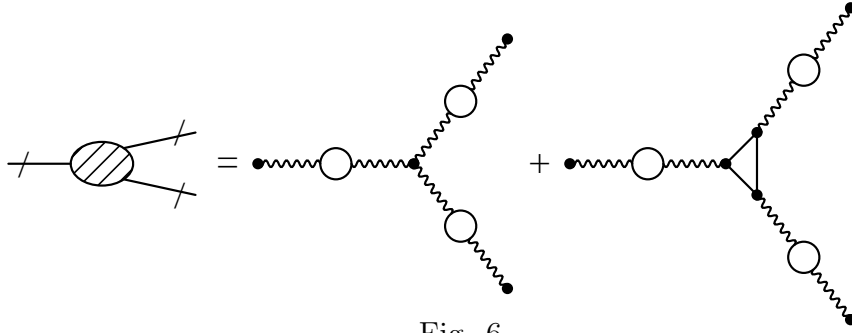


Fig. 6

where the non-factorizable three-point function $T_{\text{n.f.}}$ is given by Fig. 7

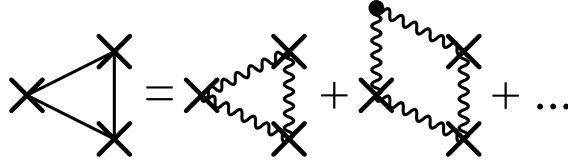


Fig. 7

The actual validity of (28), Fig. 6 has to be checked by a closer inspection of the Feynman graphs (it is just tedious combinatorics).

We find that the non-factorizable n -point functions in our theory play a role analogous to the 1PI Green functions in other theories.

The four-point function $M^{(4)}$ may be treated along similar lines. Again, the Dyson-Schwinger equation allows to express $M^{(4)}$ in terms of $\langle P \dots \rangle_m^c$ and $\langle S \dots \rangle_m^c$ n -point functions, which we do not display (the explicit expression is written down in [32]). Further, $M^{(4)}$ may be reexpressed in terms of non-factorizable n -point functions and reads

$$M^{(4)}(p_1, \dots, p_4) = (4\pi)^2 P_i P_j P_k P_l \Pi_{ii'}(p_1) \Pi_{jj'}(p_2) \Pi_{kk'}(p_3) \Pi_{ll'}(p_4) \left[\mathcal{G}_{i'j'k'l'} \right. \\ \left. + \mathcal{G}_{i'm} \mathcal{G}_{j'm'} \mathcal{G}_{k'n} \mathcal{G}_{l'n'} R_{mm'nn'}^{\text{n.f.}}(p_1, p_2, p_3, p_4) \right. \\ \left. + \left(\mathcal{G}_{i'j'm} (\Pi_{mm'}(p_1 + p_2) - \delta_{mm'}) \delta_{m'k'l'} + \text{perm.} \right) \right]$$

$$\begin{aligned}
& + \left(\mathcal{G}_{i'j'm} \Pi_{mm'}(p_1 + p_2) T_{m'nn'}^{\text{n.f.}}(p_1 + p_2, p_3, p_4) \mathcal{G}_{nk'} \mathcal{G}_{n'l'} + \text{perm.} \right) \\
& + \left(\mathcal{G}_{i'm} \mathcal{G}_{j'm'} T_{mm'n}^{\text{n.f.}}(p_1 + p_2, p_1, p_2) \mathcal{G}_{nn'} \Pi_{n'r}(p_1 + p_2) T_{rr's}^{\text{n.f.}}(p_3 + p_4, p_3, p_4) \mathcal{G}_{r'k'} \mathcal{G}_{sl'} + \text{perm.} \right) \Big] \\
& \tag{29}
\end{aligned}$$

where momentum conservation requires $p_1 + p_2 = p_3 + p_4$. Graphically, this identity may be depicted like in Fig. 8.

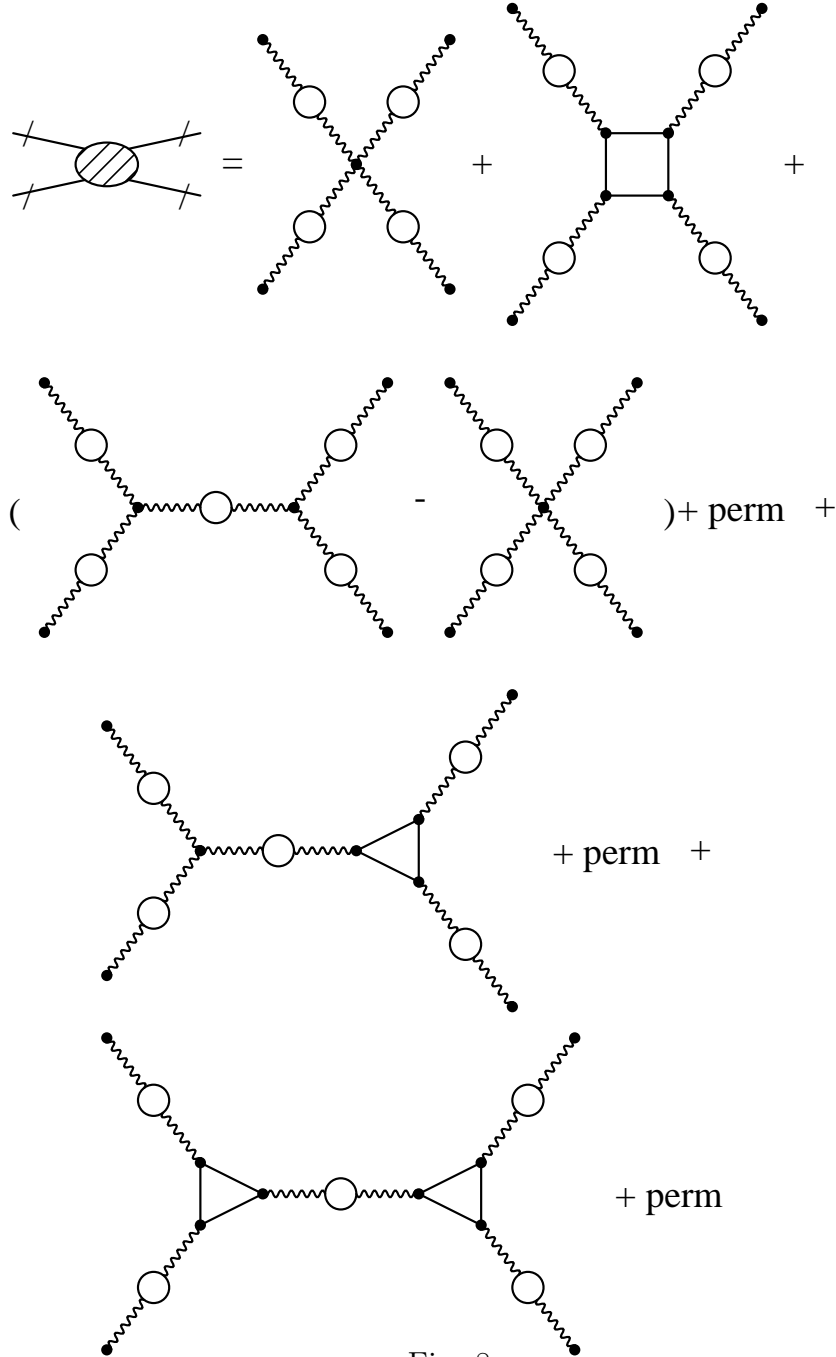


Fig. 8

The permutations in Fig. 8 contain all attachments of the external $\Pi(p_i)$ lines that are topologically distinct (i.e. 3, 6 and 3 permutations).

Observe that in each of the third type diagrams of Fig. 8 the lowest order diagram has to be subtracted in order to avoid an overcounting (this is so because $\Pi(p)$ contains the lowest order, $\mathcal{G}\Pi(p) = \mathcal{G} + o(g_\theta^2)$).

IV. BOUND-STATE STRUCTURE

Before turning to the actual scattering processes we should shortly discuss some other physical properties of the model. Actually quite a lot of physical information may be obtained from the two-point function $\Pi(p)$, (19), Fig. 2b. First, observe that the $\Pi(p)$ propagator also occurs in higher bosonic n -point functions. E.g. for $M^{(4)}$ (Fig. 8), when one takes the third type of diagrams and inserts the lowest order ($\Pi \sim \mathbf{1}$) for the four *external* $\Pi(p_i)$ lines, there remains precisely an internal $\Pi(p_1 + p_2)$ propagator (times \mathcal{G}). Therefore it is not a surprize that we can provide information on higher bosonic states, too, from $\Pi(p)$. In fact, most of the information may be inferred from the denominator $N(p)$, (20), of $\Pi(p)$. The zeros of the real part of $N(p)$ will give all the bound-state masses of the theory – at least in leading order – and the imaginary parts will give the corresponding decay widths, as was discussed in [32,35,36]. We give a short review of these results, because we need them in the sequel. The denominator $N(p)$ depends on two functions α, β , which are in lowest order

$$\alpha(g_\theta, p) = g_\theta \tilde{E}_+(p) \quad , \quad \beta(g_\theta, p) = g_\theta \tilde{E}_-(p) \quad , \quad g_\theta = m \frac{\Sigma}{2} e^{i\theta} \quad (30)$$

and the $\tilde{E}_\pm(p)$ are the exponentials of bosonic propagators,

$$\tilde{E}_\pm(p) = \sum_{n=1}^{\infty} (\pm 1)^n d_n(p) \quad , \quad d_n(p) := \frac{(4\pi)^n}{n!} \widetilde{D}_{\mu_0}^n(p). \quad (31)$$

The higher order terms which we ignored in (30) have some important effects on the lowest order expression (31) that may not be ignored. First, they cause corrections on the individual boson lines in (31) that shift all the internal bosons from the bare Schwinger mass μ_0 to the physical Schwinger mass μ (to be displayed in the next section; actually this shift does not occur for the one-boson part of $\tilde{E}_\pm(p)$, $d_1(p)$, because mass corrections to $d_1(p)$ are given by factorizable graphs that are excluded from α, β , see [32]). Therefore we redefine the $d_n(p)$ ($n \geq 2$) for the rest of the paper to be

$$d_n(p) := \frac{(4\pi)^n}{n!} \widetilde{D}_\mu^n(p). \quad (32)$$

The $d_n(p)$ are just n -boson blobs (see Fig. 9 for d_2, d_3)

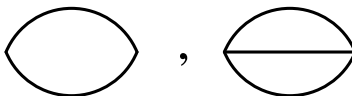


Fig. 9

and have the following properties: at $s = -p^2 = (n\mu)^2$, $d_n(p)$ has a singularity (real particle production threshold), and above this threshold it has an imaginary part. Therefore,

slightly below the threshold $(n\mu)^2$, $d_n(p)$ is large enough to balance the coupling constant and make the real part of $N(p)$, (20), vanish,

$$m\Sigma \cos \theta d_n(p) \sim 1 + o(m) \quad (33)$$

and, therefore, causes an n -boson bound state. At the position of the two-boson bound state, $s = M_2^2 = 4\mu^2 - \Delta_2$, $N(p)$ has no imaginary part and, therefore, the two-boson bound state is stable. At the three-boson bound-state mass M_3 , $d_2(s = M_3^2)$ has an imaginary part and, therefore, a decay into two Schwinger bosons (with mass μ) is possible. For higher n -boson bound states the functions d_2, \dots, d_{n-1} have imaginary parts at M_n^2 , therefore decays into $2, \dots, n - 1$ Schwinger bosons are possible ([32,35,36]).

However, this can not yet be the whole story. To understand why, look at the lowest order contribution to the three-point function, Fig. 6, with one incoming $\Pi(p_1)$, one vertex and two outgoing $\Pi(p_2)$, $\Pi(p_3)$. Suppose the incoming $\Pi(p_1)$ is at the mass $-p_1^2 = M_n^2$ of a sufficiently heavy unstable bound state. For a decay into stable final particles all the stable mass poles of $\Pi(p_2)$, $\Pi(p_3)$ are possible. But by our above arguments the mass pole of the stable M_2 particle is present in $\Pi(p_i)$ as well as the mass pole of the Schwinger boson μ . Therefore, Fig. 6 describes decays into M_2 particles as well as μ particles. On the other hand, we did not find imaginary parts (up to now) in $N(p)$ that describe decays into some M_2 , so obviously something is missing.

The M_2 bound state itself was found by a resummation, therefore it is a reasonable idea to use the higher order contributions to α , β for a further resummation. α and β are just components of the non-factorizable propagator $\mathcal{A}(p)$, (16), so let us investigate it more closely.

By a partial resummation we may find the following contribution to $\mathcal{A}(p)$,

$$H_{ii'}(p) := \int \frac{d^2q}{(2\pi)^2} \delta_{ijk} \mathcal{A}_{jj'}(q) \mathcal{G}_{j'l} \Pi_{ll'}(q) \mathcal{A}_{l'k'}(q) \mathcal{A}_{km}(q-p) \delta_{i'k'm}. \quad (34)$$

This is just a blob where $\mathcal{A}(q-p)$ runs along one line, the other terms run along the other line. We want to discuss the μ - M_2 contribution, therefore we substitute $\mathcal{A}(q-p)$ by its lowest order, one-boson part,

$$\mathcal{A}(q-p) \sim 4\pi \widetilde{D}_\mu(q-p) \begin{pmatrix} 1 & -1 \\ -1 & 1 \end{pmatrix} \quad (35)$$

and the two further $\mathcal{A}(q)$ by their lowest order contribution

$$\mathcal{A}(q) \sim \begin{pmatrix} \widetilde{E}_+(q) & \widetilde{E}_-(q) \\ \widetilde{E}_-(q) & \widetilde{E}_+(q) \end{pmatrix} \quad (36)$$

The resummation that we need in (34) is taken into account by $\Pi(q)$. With these restrictions $H(p)$ corresponds to the graph of Fig. 10

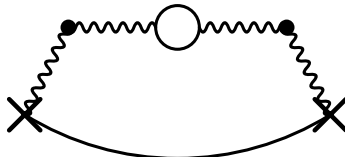


Fig. 10

Observe that all internal bosons may be renormalized to their physical masses μ , because this does not spoil non-factorizability in Fig. 10. The two factors $\mathcal{A}(q)$ in (34) are necessary in order to avoid an overcounting, but they cannot influence the presence of higher poles in Fig. 10.

Now suppose that $H(p)$ is at the $M_2 + \mu$ -threshold, $s = -p^2 = (M_2 + \mu)^2$. Then $\widetilde{D}_\mu(q-p)$ is at its μ -singularity and $\Pi(q)$ at its M_2 -singularity, and Fig. 10 corresponds (up to a normalization) to a μ - M_2 two-boson loop, i.e. Fig. 10 may effectively be substituted by Fig. 11,

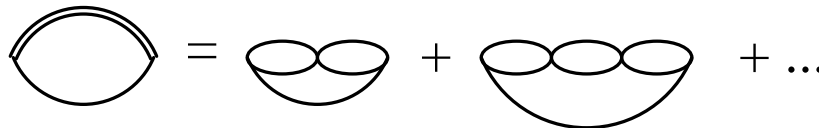


Fig. 11

where the double line represents the two-boson bound-state propagator.

Therefore, $H(p)$ is singular at $-p^2 = (M_2 + \mu)^2$, and has a large real part slightly below and a large imaginary part slightly above this threshold. As a consequence, when the contribution of $H(p)$ to $\alpha(p)$ is taken into account in the denominator $N(p)$, (20), it will give rise to a further μ - M_2 bound state slightly below $s = (M_2 + \mu)^2$. Further it will open the μ - M_2 decay channel at $s = (M_2 + \mu)^2$.

Now suppose we put $\Pi(q)$ in (34) on a higher (unstable) bound-state mass M_n , $n > 2$. Then in the denominator $N(q)$ of $\Pi(q)$ (see (20)) the real part again vanishes, but there remains an imaginary part. Therefore, $H(p)$ is finite and imaginary at $s = -p^2 = (M_n + \mu)^2$ and *cannot* give rise to a μ - M_n bound-state formation.

Further, because there is no threshold singularity at $s = (M_n + \mu)^2$, this means that *no* new decay channel opens at that point (i.e. the imaginary part of $H(p)$ varies smoothly around $s \sim (M_n + \mu^2)$), which simply means that the unstable higher n -boson bound states are no possible final states (of course, they are possible as intermediate resonances).

We could substitute the one-boson line in Fig. 10 by another $\mathcal{AG}\Pi\mathcal{A}$ line and would find that this graph behaves like a M_2 - M_2 blob near $s = (M_2 + M_2)^2$, and we could allow for even more $\mathcal{AG}\Pi\mathcal{A}$ lines. The physical picture that evolves from these considerations is like follows: in addition to the unstable n -boson bound states there exist further (unstable) bound states that are composed of Schwinger bosons μ and (stable) two-boson bound states M_2 . Further, the unstable bound states may decay into all combinations of μ and M_2 particles that are possible kinematically. The imaginary parts of the corresponding n -particle blobs (where particle means μ or M_2) are large near their thresholds, therefore there is a kinematical tendency to rise the decay probabilities for decays with *small* kinetic energy. This is not so surprising, because in 1 + 1 dimensions the phase space "volume" does not grow with kinetic energy.

V. BOUND-STATE MASSES AND DECAY WIDTHS

Up to now we discussed the physical properties of the model on a qualitative level, but for the further discussion we need some explicit results, too.

The mass pole equation in lowest order reads

$$1 = (g_\theta + g_\theta^*) \text{Re} \tilde{E}_+(p) \quad (37)$$

or, for the n -boson bound state

$$f_n(p) := 1 - m\Sigma \cos \theta d_n(p) = 0 \quad (38)$$

and has the three lowest solutions ($n = 1, 2, 3$; we only display the leading order corrections)

$$M_1^2 \equiv \mu^2 = \mu_0^2 + \Delta_1 \quad , \quad \Delta_1 = 4\pi m\Sigma \cos \theta \quad (39)$$

$$M_2^2 = 4\mu^2 - \Delta_2 \quad , \quad \Delta_2 = \frac{4\pi^4 m^2 \Sigma^2 \cos^2 \theta}{\mu^2} \quad (40)$$

$$M_3^2 = 9\mu^2 - \Delta_3 \quad , \quad \Delta_3 \simeq 6.993\mu^2 \exp(-0.263 \frac{\mu^2}{m\Sigma \cos \theta}) \quad (41)$$

(these masses have already been computed in [32]; there is, however, a numerical error in the M_2 mass formula in [32]). The $f_n(p)$ of (38) may be expanded in Taylor series about their respective mass poles $s = M_n^2$. The leading coefficients ($s = -p^2$)

$$f_n(p) \simeq c_n(s - M_n^2) \quad (42)$$

which we need for the residues of the mass poles, are (see [36] for a computation)

$$c_1 = \frac{1}{4\pi m\Sigma \cos \theta} = \frac{1}{\Delta_1} \quad (43)$$

$$c_2 = \frac{\mu^2}{8\pi^4(m\Sigma \cos \theta)^2} = \frac{1}{2\Delta_2} \quad (44)$$

$$c_3 = \frac{m\Sigma \cos \theta}{0.263\mu^2\Delta_3} \quad (45)$$

The next things we need are the residues of the propagator $\Pi(p)$ at the two lowest mass poles. Inserting the lowest order ($\alpha \sim g_\theta \tilde{E}_+$ etc.) into formula (19) and using the pole equation (38) we find at once (here $n = 1, 2$)

$$\Pi(s \sim M_n^2) \sim \frac{1}{(g_\theta + g_\theta^*)c_n(s - M_n^2)} \begin{pmatrix} g_\theta & (-1)^n g_\theta^* \\ (-1)^n g_\theta & g_\theta^* \end{pmatrix} \quad (46)$$

For the computation of the μ - M_2 bound state we need, in addition, the matrix \mathcal{A} , (16), at the n -boson mass poles (here $n \neq 1$, because there \mathcal{A} itself has a pole (46)),

$$\mathcal{A}(s = M_n^2) = \frac{1}{g_\theta + g_\theta^*} \begin{pmatrix} 1 & (-1)^n \\ (-1)^n & 1 \end{pmatrix} \quad (47)$$

Using these results we find for the matrix $H(p)$, (34), near the μ - M_2 threshold

$$\begin{aligned}
H_{ii'}(-p^2 \sim (M_2 + \mu)^2) &\sim \int \frac{d^2q}{(2\pi)^2} \delta_{ijk} \frac{1}{g_\theta + g_\theta^*} \begin{pmatrix} 1 & 1 \\ 1 & 1 \end{pmatrix}_{jj'} \begin{pmatrix} g_\theta & 0 \\ 0 & g_\theta^* \end{pmatrix}_{j'l} \frac{1}{(g_\theta + g_\theta^*)c_2(-q^2 - M_2^2)} \\
&\cdot \begin{pmatrix} g_\theta & g_\theta^* \\ g_\theta & g_\theta^* \end{pmatrix}_{ll'} \frac{1}{g_\theta + g_\theta^*} \begin{pmatrix} 1 & 1 \\ 1 & 1 \end{pmatrix}_{l'k'} \frac{1}{(g_\theta + g_\theta^*)c_1(-(q-p)^2 - \mu^2)} \begin{pmatrix} 1 & -1 \\ -1 & 1 \end{pmatrix}_{km} \delta_{i'k'm} = \\
\delta_{ijk} \begin{pmatrix} 1 & 1 \\ 1 & 1 \end{pmatrix}_{jj'} \begin{pmatrix} 1 & -1 \\ -1 & 1 \end{pmatrix}_{kk'} \delta_{i'j'k'} \int \frac{d^2q}{(2\pi)^2} \frac{1}{(g_\theta + g_\theta^*)^2 c_1 c_2 (-q^2 - M_2^2) (-(q-p)^2 - \mu^2)} \quad (48)
\end{aligned}$$

The contribution of $H_{ii'}$ to $\alpha(g_\theta) + \alpha(g_\theta^*)$ in the denominator $N(p)$, (20), is

$$\begin{aligned}
g_\theta H_{++}(p) + g_\theta^* H_{--}(p) &=: (g_\theta + g_\theta^*) d_{1,1}(p) = \\
(g_\theta + g_\theta^*) \int \frac{d^2q}{(2\pi)^2} \frac{8\pi^4 m \Sigma \cos \theta}{\mu^2 (q^2 + M_2^2)} \frac{4\pi}{(p-q)^2 + \mu^2} = \\
\frac{32\pi^5 m^2 \Sigma^2 \cos^2 \theta}{2\pi \mu^2 \bar{w}(s, M_2^2, \mu^2)} \left(\pi + \right. \\
\left. \arctan \frac{2s}{\bar{w}(s, M_2^2, \mu^2) - \frac{1}{\bar{w}(s, M_2^2, \mu^2)} (s + \mu^2 - M_2^2)(s - \mu^2 + M_2^2)} \right) \quad (49)
\end{aligned}$$

$$\bar{w}(x, y, z) := (-x^2 - y^2 - z^2 + 2xy + 2xz + 2yz)^{\frac{1}{2}} \quad (50)$$

where $s = -p^2 \sim (\mu + M_2)^2$. The μ - M_2 bound-state mass fulfills the equation

$$1 = (g_\theta + g_\theta^*) d_{1,1}(p) \quad (51)$$

with the solution in leading order (here $M_{1,1}$ denotes the μ - M_2 bound-state mass)

$$M_{1,1}^2 = (\mu + M_2)^2 - \Delta_{1,1} \quad , \quad \Delta_{1,1} = \frac{32\pi^{10} (m \Sigma \cos \theta)^4}{\mu^6} \quad (52)$$

which is valid for sufficiently small $\Delta_{1,1}$. $M_{1,1}$ was computed from a two-boson blob (Fig. 11), like M_2 , therefore the Taylor coefficient of $(s - M_{1,1}^2)$ is analogous to c_2 , equ. (44),

$$c_{1,1} = \frac{1}{2\Delta_{1,1}} = \frac{\mu^6}{64\pi^{10} (m \Sigma \cos \theta)^4}. \quad (53)$$

Further, the above equ. (48) shows that the μ - M_2 blob $d_{1,1}(p)$ enters into the functions α, β of \mathcal{A} , (16), like any other odd n -boson blob $d_n(p)$ ($d_{1,1}(p)$ consists of three Schwinger bosons and is, therefore, parity odd).

In the sequel we will be interested in the behaviour of the exact two-point function $\Pi(p)$, equ. (19), and its denominator $N(p)$ in the vicinity of the mass poles $s \sim M_n^2$. Using the first order approximation (30) for α, β we find for $N(p)$ (e.g. in the vicinity of $s \sim M_3^2$ for definiteness)

$$\begin{aligned} N(p) &\simeq 1 - m\Sigma \cos \theta \tilde{E}_+(p) + \frac{m^2 \Sigma^2}{4} (\tilde{E}_+^2(p) - \tilde{E}_-^2(p)) \\ &= 1 - m\Sigma \cos \theta (d_1(p) + d_2(p) + d_{1,1}(p) + d_3(p) + \dots) + \\ &\quad m^2 \Sigma^2 (d_1(p)(d_2(p) + d_4(p) + \dots) + d_{1,1}(p)(d_2(p) + d_4(p) + \dots) + \\ &\quad d_3(p)(d_2(p) + d_4(p) + \dots) + \dots) \end{aligned} \quad (54)$$

where we included the μ - M_2 blob $d_{1,1}$, as discussed above, because we need it for the subsequent discussion (we ignore, for the moment, higher M_2 blobs that are, in principle, present). Near $s = M_3^2$ the real part of (54) is given by $c_3(s - M_3^2)$ and we find

$$\begin{aligned} N(p) &\sim c_3(s - M_3^2) - im\Sigma \cos \theta (\text{Im}d_2(s \sim M_3^2) + \text{Im}d_{1,1}(s \sim M_3^2)) + \\ &\quad im^2 \Sigma^2 d_3(s \sim M_3^2) \text{Im}d_2(s \sim M_3^2) + o(m^2) \\ &= c_3(s - M_3^2) - im\Sigma (\cos \theta - \frac{1}{\cos \theta}) \text{Im}d_2(M_3^2) - im\Sigma \cos \theta \text{Im}d_{1,1}(M_3^2) + o(m^2) \end{aligned} \quad (55)$$

where we used $d_3(M_3^2) \sim \frac{1}{m\Sigma \cos \theta}$, see (38).

This computation may be generalized and tells us that parity forbidden imaginary parts (decay channels) acquire a factor $(\cos \theta - \frac{1}{\cos \theta})$, whereas parity allowed imaginary parts have the usual $\cos \theta$ factor.

Remark: There seems to be something wrong with the sign of the parity forbidden imaginary part (the d_2 term). Actually the sign is o.k. and the problem is a remnant of the Euclidean conventions that are implicit in the whole computation (see e.g. [12,21]). In these conventions θ is imaginary and therefore $(\cos \theta - \frac{1}{\cos \theta}) \geq 0$. Of course, this is not a reasonable convention for a final result. When performing the whole computation in Minkowski space and for real θ , roughly speaking, the roles of E_+ and E_- are exchanged in (54). This gives an additional relative sign between parity even and odd n -boson propagators and, therefore, changes the factor of d_2 to $(\frac{1}{\cos \theta} - \cos \theta)$, which is ≥ 0 for real θ . We will keep this remark in mind and express the final results in Minkowski space and for real θ .

From the imaginary parts of (55) one is able to compute the partial decay widths of the three-boson bound state, and in a similar way one may compute the decay widths of the other unstable bound states (see [35,36]). The explicit results for the M_3 and $M_{1,1}$ decay widths read (in Minkowski space and for real θ)

$$\Gamma_{M_{1,1} \rightarrow 2\mu} = \frac{2^8 \pi^{12} (m\Sigma \cos \theta)^5}{9\sqrt{5}\mu^9} (\frac{1}{\cos^2 \theta} - 1) \simeq 21340\mu (\frac{m \cos \theta}{\mu})^5 (\frac{1}{\cos^2 \theta} - 1) \quad (56)$$

$$\Gamma_{M_3 \rightarrow 2\mu} = 0.263 \frac{4\pi^2 \Delta_3}{9\sqrt{5}\mu} (\frac{1}{\cos^2 \theta} - 1) \simeq 3.608\mu (\frac{1}{\cos^2 \theta} - 1) \exp(-0.929 \frac{\mu}{m \cos \theta}) \quad (57)$$

$$\Gamma_{M_3 \rightarrow M_2 + \mu} = 0.263 \frac{4\pi^3 \Delta_3}{3\sqrt{3}\mu} \simeq 43.9\mu \exp(-0.929 \frac{\mu}{m \cos \theta}) \quad (58)$$

We will need expression (55) for our scattering discussion.

VI. TWO-DIMENSIONAL KINEMATICS

Next we need some basic facts about two-dimensional kinematics. We will restrict our discussion to elastic scattering. Suppose we have two incoming particles with masses M_1 , M_2 and momenta p_1 , p_2 , and two outgoing particles, again with masses M_1 , M_2 , and with momenta p_3 , p_4 . Momentum conservation requires

$$p := p_1 + p_2 = p_3 + p_4 \quad (59)$$

and all momenta are *Minkowskian* in the sequel. In the center of mass system we may write

$$\begin{aligned} p_1 &= \begin{pmatrix} \sqrt{k^2 + M_1^2} \\ k \end{pmatrix}, & p_2 &= \begin{pmatrix} \sqrt{k^2 + M_2^2} \\ -k \end{pmatrix} \\ p_3 &= \begin{pmatrix} \sqrt{k^2 + M_1^2} \\ \pm k \end{pmatrix}, & p_4 &= \begin{pmatrix} \sqrt{k^2 + M_2^2} \\ \mp k \end{pmatrix} \end{aligned} \quad (60)$$

where in p_3 , p_4 the first sign is for transmission, the second sign is for reflexion. For the kinematical variables we find for transmission

$$\begin{aligned} s &= (p_1 + p_2)^2 = 2k^2 + M_1^2 + M_2^2 + 2\sqrt{(k^2 + M_1^2)(k^2 + M_2^2)} \\ t_T &= (p_1 - p_4)^2 = -2k^2 + M_1^2 + M_2^2 - 2\sqrt{(k^2 + M_1^2)(k^2 + M_2^2)} \\ u_T &= (p_1 - p_3)^2 = 0 \end{aligned} \quad (61)$$

and for reflexion

$$\begin{aligned} s &= (p_1 + p_2)^2 = 2k^2 + M_1^2 + M_2^2 + 2\sqrt{(k^2 + M_1^2)(k^2 + M_2^2)} \\ t_R &= (p_1 - p_4)^2 = 2k^2 + M_1^2 + M_2^2 - 2\sqrt{(k^2 + M_1^2)(k^2 + M_2^2)} \\ u_R &= (p_1 - p_3)^2 = -4k^2 \end{aligned} \quad (62)$$

When the two masses are equal, the two particles are identical in our theory and the discrimination between transmission and reflexion does not make sense. The kinematical variables turn into

$$\begin{aligned} s &= (p_1 + p_2)^2 = 4(k^2 + M^2) \\ t &= (p_1 - p_4)^2 = -4k^2 \\ u &= (p_1 - p_3)^2 = 0 \end{aligned} \quad (63)$$

The elastic scattering cross section of two particles is given by

$$\sigma_{M_a M_b \rightarrow M_a M_b}(s) = \frac{C_{\text{sym}} |\mathcal{M}(s)|^2}{2w^2(s, M_a^2, M_b^2)} \quad (64)$$

$$w(x, y, z) = (x^2 + y^2 + z^2 - 2xy - 2xz - 2yz)^{\frac{1}{2}} \quad (65)$$

where \mathcal{M} is the transition matrix element and C_{sym} is a symmetry factor that takes into account identical particles in the final state ($C_{\text{sym}} = \frac{1}{n_1!n_2!}$ for n_1 particles M_1 and n_2 particles M_2 in the final state). As it stands, expression (64) holds provided that the initial and final particle propagators are normalized in the usual fashion ($\sim \frac{1}{s-M_i^2}$). Otherwise, (64) is multiplied by the normalization factors (the residues of the propagators).

Unitarity relates the scattering cross section to the imaginary parts of some graphs, therefore let us write down the imaginary part of the two-boson blob for later convenience,

$$\begin{aligned} \text{Im}(D_{M_1}\widetilde{D}_{M_2})(s) &= \text{Im} \int \frac{d^2q}{(2\pi)^2} \frac{-1}{q^2 + M_1^2} \frac{-1}{(p-q)^2 + M_2^2} \\ &= \frac{1}{2w(s, M_1^2, M_2^2)} \end{aligned} \quad (66)$$

VII. SCATTERING PROCESSES

Finally we are prepared for a discussion of scattering. Let us focus for the moment on the lowest order graph of Fig. 8 for the four-point function (29). It consists of four external exact propagators $\Pi(p_i)$ and a simple vertex as the lowest order transition matrix element. The $\Pi(p_i)$ contain two stable-particle mass poles, μ and M_2 , therefore this graph describes μ and M_2 scattering (this remains true for higher order contributions; as a consequence, the same transition matrix elements contribute to μ and M_2 scattering processes, and they may only differ by some kinematical and normalization factors).

Let us consider elastic scattering of two Schwinger bosons for definiteness. Then each external $\Pi(p_i)$ propagator is odd and contributes to the graph like ($s_i = -p_i^2$)

$$\Pi_{jk}(s_i = \mu^2)P_k = \frac{4\pi(g_\theta + g_\theta^*)}{s_i - \mu^2} \begin{pmatrix} 1 \\ -1 \end{pmatrix}_j \quad (67)$$

Here we face the problem that the first graph of Fig. 8 is already of fifth order, because each propagator $\Pi(s_i)$ has an external vertex. We just omit these external vertices (i.e. we omit the factor $(g_\theta + g_\theta^*)$ in (67) for each propagator), because we want to discuss first order scattering. Doing so, we find for this graph

$$P_{j_1}P_{j_2}P_{j_3}P_{j_4}\delta_{j_1j_2k_1}\mathcal{G}_{k_1k_2}\delta_{j_3j_4k_2}\prod_{i=1}^4\frac{4\pi}{s_i - \mu^2} = (g_\theta + g_\theta^*)\prod_{i=1}^4\frac{4\pi}{s_i - \mu^2} \quad (68)$$

i.e. each μ propagator has a residue 4π . In order to obtain the transition matrix element one has to amputate the external boson propagators in the usual LSZ fashion. When the propagators are normalized by $r_1 = 4\pi$, the bosons themselves are normalized by $\sqrt{4\pi}$, which has to be divided out for each amputation. This leaves a factor $\sqrt{4\pi}$ for each external boson in the transition matrix element. However, the squared transition matrix element enters the scattering cross section, therefore the net effect on the cross section is a multiplication by the corresponding propagator residue r_i for each external line (here $r_1 = 4\pi$).

Therefore, we find for the lowest order boson-boson elastic scattering

$$\sigma_{\mu+\mu\rightarrow\mu+\mu}(s) = r_1^4 \frac{\frac{1}{2}(m\Sigma \cos \theta)^2}{2w^2(s, \mu^2, \mu^2)} \quad , \quad r_1 = 4\pi \quad (69)$$

which, of course, coincides with a naive computation using the first order bosonic four-point function $\langle \Phi(x_1) \dots \Phi(x_4) \rangle_m^c$ (the latter may be inferred immediately from (4)). Observe that (69) is singular at the real particle production threshold $s = 4\mu^2$ ($w(4\mu^2, \mu^2, \mu^2) = 0$).

In a next step we want to consider the second order contribution of Fig. 8 (the third type graphs). There are three graphs of this type, namely s , t and u channel, but we will consider only the s channel (annihilation channel) for the moment. In this diagram the lowest order graph must be subtracted in order to avoid overcounting (see Fig. 8), therefore the graph of Fig. 12

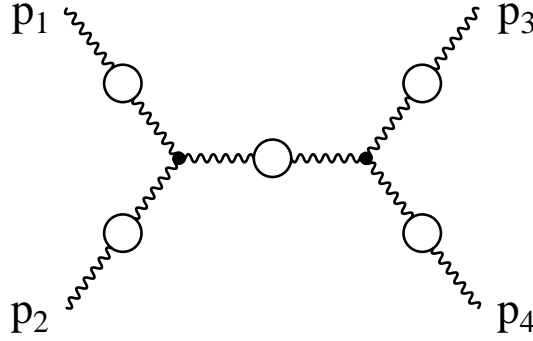


Fig. 12

contains the lowest order graph and the second order s channel contribution.

Actually we will allow for arbitrary final states in the sequel, $\mu + \mu \rightarrow f$, because this enables us to use the optical theorem, which may be written for the current problem like

$$\sigma_{ab\rightarrow f}^{\text{tot}}(s) = \frac{r_a r_b}{w(s, M_a^2, M_b^2)} \text{Im} \mathcal{M}_{ab\rightarrow ab}(s) \quad (70)$$

where the r_i are the propagator residues (46) and $\mathcal{M}_{ab\rightarrow ab}$ is the forward elastic scattering amplitude. $w(s, M_a^2, M_b^2)$ is an initial state velocity factor; the final state factors must be produced by $\mathcal{M}_{ab\rightarrow ab}$, as we will find in the sequel.

Specifically we choose $a = b = \mu$, and, therefore, both vertices of \mathcal{M} are contracted by scalars S (we use matrix notation)

$$\mathcal{M}_{2\mu\rightarrow 2\mu}(s) = S^T \mathcal{G} \Pi(s) S \quad (71)$$

Before starting the computations, we want to make some comments. First, as is obvious from Fig. 12 and our discussion, in (70) all combinations of $n_1\mu$ and n_2M_2 are allowed as final states. Consequently, they must exist as intermediate states in $\mathcal{M}_{2\mu\rightarrow 2\mu}$, too, in order to saturate the optical theorem (70). Therefore, we are forced to include the M_2 particle into the two-point function $\Pi(p)$, as we did in the previous section, in order to maintain unitarity.

Secondly, in finite order perturbation theory the optical theorem relates graphs of different order. However, we use a resummed perturbation series in (70) and, therefore, we will find a relation that holds for the whole, resummed two-point function $\Pi(s)$.

In a first step we want to discuss the special case $\theta = 0$, because it is much easier and shows the relevant features without technical complications. For $\theta = 0$ the amplitude (71) reads (see [32] for an extensive discussion of the $\theta = 0$ case)

$$\begin{aligned}\mathcal{M}_{2\mu \rightarrow 2\mu}^{\theta=0}(s) &= \frac{m\Sigma}{1 - \frac{m\Sigma}{2}(\tilde{E}_+(s) + \tilde{E}_-(s))} \\ &= \frac{m\Sigma}{1 - m\Sigma(d_2(s) + d_{2,0}(s) + d_4(s) + \dots)}\end{aligned}\quad (72)$$

where we inserted the lowest order (30) and expanded the exponentials $\tilde{E}_{\pm}(s)$ like in (31). Again, we include the M_2 particle (which is found by a further resummation) into \tilde{E}_{\pm} , because this is absolutely necessary, as we have just argued. Actually $d_{2,0}$ describes the M_2 - M_2 blob, and in (72) only parity even contributions may occur. For the optical theorem (70) we need the imaginary part

$$\text{Im}\mathcal{M}_{2\mu \rightarrow 2\mu}^{\theta=0}(s) = \frac{m^2\Sigma^2(\text{Im}d_2(s) + \text{Im}d_{2,0}(s) + \text{Im}d_4(s) + \dots)}{[1 - m\Sigma(\text{Re}d_2(s) + \dots)]^2 + m^2\Sigma^2(\text{Im}d_2(s) + \dots)^2}\quad (73)$$

We find the following physical picture: at $s = 4\mu^2$ the elastic scattering threshold ($f = 2\mu$) opens, at $s = 4M_2^2$ the $2\mu \rightarrow 2M_2$ threshold is added, at $s = 16\mu^2$ the $2\mu \rightarrow 4\mu$ threshold, etc. The $d_n(s)$ were defined as $d_n(s) = \frac{r_1^n}{n!}\tilde{D}_\mu^n(s)$, therefore their imaginary parts are precisely the final state factors for the corresponding cross section, including the phase space integration (the cutting of the $\tilde{D}_\mu^n(s)$), the propagator normalizations $r_1 = 4\pi$, and the final state symmetry factors for n identical particles, $C_{\text{sym}} = \frac{1}{n!}$. For the multi- M_2 propagators $d_{m,0}(s)$ (and, more generally, for $d_{m,n}(s)$) the first two points (propagators with their residues) are obvious, the third one (correct $\frac{1}{m!}$ final state symmetry factor) may be checked by a closer inspection of the mass perturbation series. We show it for the lowest order contribution to the M_2 - M_2 propagator $d_{2,0}(s)$, where we depict in Fig. 13 this lowest order contribution and the perturbation expansion graph where it stems from

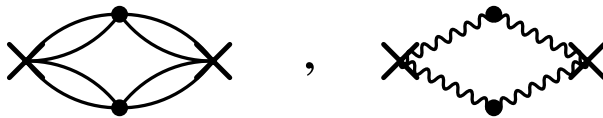


Fig. 13

The second graph in Fig. 13 is a second order mass perturbation, therefore it contains a factor $\frac{m^2}{2!}$. Further there exists precisely one diagram of this kind in the perturbation series, therefore the $\frac{1}{2!}$ factor remains in $d_{2,0}(s)$ as the required final space symmetry factor. Via some combinatorics this argument may be generalized to higher order contributions to the M_2 - M_2 loop $d_{2,0}(s)$ and to higher multi- M_2 loops.

For the total cross section (70) we get

$$\sigma_{2\mu \rightarrow f}^{\text{tot},\theta=0}(s) = \frac{r_1^2 m^2 \Sigma^2 (\text{Im}d_2(s) + \text{Im}d_{2,0}(s) + \text{Im}d_4(s) + \dots)}{w(s, \mu^2, \mu^2) \left([1 - m\Sigma(\text{Re}d_2(s) + \dots)]^2 + m^2 \Sigma^2 (\text{Im}d_2(s) + \dots)^2 \right)}\quad (74)$$

$$\text{Im}d_2(s) = \frac{r_1^2}{2!} \frac{1}{2w(s, \mu^2, \mu^2)} \quad \text{etc.}\quad (75)$$

which we want to evaluate for some specific values of s . At the elastic scattering threshold $s = 4\mu^2$, $\text{Im}d_2(s)$ is singular and we find

$$\sigma_{2\mu \rightarrow f}^{\text{tot}, \theta=0}(4\mu^2) = 4. \quad (76)$$

Therefore, the singular behaviour of the lowest order cross section at $s = 4\mu^2$ is cancelled by higher order contributions. This behaviour is, however, further changed by the t and u channel contributions.

In an intermediate range, far from all thresholds and bound state masses, $4\mu^2 < s < 4M_2^2$, σ^{tot} is well described by the lowest order result (69), because there $m\Sigma d_n(s)$ is small compared to 1,

$$\sigma_{2\mu \rightarrow f}^{\text{tot}, \theta=0}(s) \simeq \frac{r_1^2 m^2 \Sigma^2 \text{Im}d_2(s)}{w(s, \mu^2, \mu^2)} = \frac{\frac{1}{2!} r_1^4 m^2 \Sigma^2}{2w^2(s, \mu^2, \mu^2)}. \quad (77)$$

At the first bound-state mass, $s = M_{2,0}^2 < 4M_2^2$, a resonance occurs. There the real part contribution to the denominator of (74) vanishes by definition and we find

$$\sigma_{2\mu \rightarrow f}^{\text{tot}, \theta=0}(M_{2,0}^2) = \frac{r_1^2 m^2 \Sigma^2 \text{Im}d_2(M_{2,0}^2)}{w(M_{2,0}^2, \mu^2, \mu^2) m^2 \Sigma^2 (\text{Im}d_2(M_{2,0}^2))^2} = 4 \quad (78)$$

and the resonance height does not depend on the coupling constant (of course, the width does).

At the $2M_2$ production threshold $s = 4M_2^2$ the scattering cross section goes down to zero (here $d_{2,0}$ is singular)

$$\sigma_{2\mu \rightarrow f}^{\text{tot}, \theta=0}(4M_2^2) \simeq \frac{r_1^2 m^2 \Sigma^2}{w(4M_2^2, \mu^2, \mu^2)} \frac{\text{Im}d_{2,0}(4M_2^2)}{m^2 \Sigma^2 (\text{Im}d_{2,0}(4M_2^2))^2} = 0. \quad (79)$$

In addition, at this point the $2\mu \rightarrow 2M_2$ production channel opens. At the four-boson bound-state mass $s = M_4^2$ we find the next resonance

$$\sigma_{2\mu \rightarrow f}^{\text{tot}, \theta=0}(M_4^2) = \frac{r_1^2 (\text{Im}d_2(M_4^2) + \text{Im}d_{2,0}(M_4^2))}{w(M_4^2, \mu^2, \mu^2) (\text{Im}d_2(M_4^2) + \text{Im}d_{2,0}(M_4^2))^2} \quad (80)$$

Again, the resonance height does not depend on the coupling constant, and, in addition, here already two decay channels are open for the M_4 resonance.

At the $2\mu \rightarrow 4\mu$ real production threshold $s = 16\mu^2$, σ^{tot} again vanishes, and for even higher s the above pattern repeats.

Observe that, because σ^{tot} has a local maximum (resonance) at the bound-state masses, whereas it is zero at the real particle production thresholds, the resonance widths (decay widths) *must* be bounded by the binding energies. For the $M_{1,1}$ and M_3 decay widths this may be seen from the explicit results (56) – (58).

The t and u channel contributions do not change this pattern (they have no imaginary parts and are small for all t, u).

Next let us turn to the $\theta \neq 0$ case. There parity forbidden transitions are possible, and therefore we will find $M_{1,1}$ and M_3 resonances, too. The forward scattering amplitude (71) reads

$$\mathcal{M}_{2\mu \rightarrow 2\mu}(s) = \frac{g_\theta + g_\theta^* - 2g_\theta g_\theta^*(\tilde{E}_+(s) - \tilde{E}_-(s))}{1 - (g_\theta + g_\theta^*)\tilde{E}_+(s) + g_\theta g_\theta^*(\tilde{E}_+^2(s) + \tilde{E}_-^2(s))} =$$

$$\frac{g_\theta + g_\theta^* - 4g_\theta g_\theta^*(d_1(s) + d_{1,1}(s) + d_3(s) + \dots)}{1 - (g_\theta + g_\theta^*)(d_1(s) + d_2(s) + d_{1,1}(s) + \dots) + 4g_\theta g_\theta^*[d_1(s)(d_2(s) + d_{2,0}(s) + \dots) + \dots]} \quad (81)$$

Please observe the presence of only odd d_i in the numerator and of only odd \times even $d_i \times d_j$ in the second term of the denominator. Therefore, the $4g_\theta g_\theta^*$ terms in the numerator and denominator do not contribute to parity allowed transitions, and the discussion of such parity allowed transitions is analogous to the $\theta = 0$ case that we discussed above.

Again, we want to discuss the scattering cross section

$$\sigma_{2\mu \rightarrow f}^{\text{tot}}(s) = \frac{r_1^2}{w(s, \mu^2, \mu^2)} \text{Im} \mathcal{M}_{2\mu \rightarrow 2\mu}(s) \quad (82)$$

for some specific values of s . At $s = 4\mu^2$ we find again

$$\sigma_{2\mu \rightarrow f}^{\text{tot}}(4\mu^2) = \frac{r_1^2}{w(4\mu^2, \mu^2, \mu^2)} \frac{(g_\theta + g_\theta^*)^2 \text{Im} d_2(4\mu^2)}{1 + (g_\theta + g_\theta^*)^2 (\text{Im} d_2(4\mu^2))^2} = 4 \quad (83)$$

At the first parity forbidden resonance $s = M_{1,1}^2$ we find ($\text{Red}_{1,1} = \frac{1}{g_\theta + g_\theta^*}$)

$$\sigma_{2\mu \rightarrow f}^{\text{tot}}(M_{1,1}^2) \simeq \frac{r_1^2}{w(M_{1,1}^2, \mu^2, \mu^2)} \text{Im} \frac{g_\theta + g_\theta^* - 4g_\theta g_\theta^* \text{Red}_{1,1}(M_{1,1}^2)}{-i(g_\theta + g_\theta^*) \text{Im} d_2(M_{1,1}^2) + 4ig_\theta g_\theta^* \text{Red}_{1,1}(M_{1,1}^2) \text{Im} d_2(M_{1,1}^2)}$$

$$= \frac{r_1^2}{w(M_{1,1}^2, \mu^2, \mu^2)} \frac{\left(g_\theta + g_\theta^* - \frac{4g_\theta g_\theta^*}{g_\theta + g_\theta^*}\right)^2 \text{Im} d_2(M_{1,1}^2)}{\left(g_\theta + g_\theta^* - \frac{4g_\theta g_\theta^*}{g_\theta + g_\theta^*}\right)^2 (\text{Im} d_2(M_{1,1}^2))^2}$$

$$= 4 \quad (84)$$

and, therefore, the same resonance height as for the first parity allowed resonance in the $\theta = 0$ case (78).

At the parity forbidden threshold $s = (M_2 + \mu)^2$, where $\text{Im} d_{1,1}((M_2 + \mu)^2)$ is singular, we find

$$\sigma_{2\mu \rightarrow f}^{\text{tot}}((M_2 + \mu)^2) \simeq \frac{r_1^2}{w((M_2 + \mu)^2, \mu^2, \mu^2)} \cdot \text{Im} \frac{g_\theta + g_\theta^* - 4ig_\theta g_\theta^* \text{Im} d_{1,1}((M_2 + \mu)^2)}{1 - i(g_\theta + g_\theta^*)(\text{Im} d_2 + \text{Im} d_{1,1}) - 4g_\theta g_\theta^* \text{Im} d_2 \text{Im} d_{1,1}} =$$

$$\frac{r_1^2}{w((M_2 + \mu)^2, \mu^2, \mu^2)} \frac{(g_\theta + g_\theta^*)^2 (\text{Im} d_2 + \text{Im} d_{1,1}) - 4g_\theta g_\theta^* \text{Im} d_{1,1} (1 - 4g_\theta g_\theta^* \text{Im} d_2 \text{Im} d_{1,1})}{(1 - 4g_\theta g_\theta^* \text{Im} d_2 \text{Im} d_{1,1})^2 + (g_\theta + g_\theta^*)^2 (\text{Im} d_2 + \text{Im} d_{1,1})^2}$$

$$\rightarrow \frac{r_1^2}{w((M_2 + \mu)^2, \mu^2, \mu^2)} \frac{4g_\theta g_\theta^* (\text{Im} d_{1,1})^2 \text{Im} d_2}{(g_\theta + g_\theta^*)^2 (\text{Im} d_{1,1})^2} \rightarrow \left(\frac{4g_\theta g_\theta^*}{g_\theta + g_\theta^*}\right)^2 \frac{r_1^2 \text{Im} d_2 ((M_2 + \mu)^2)}{w((M_2 + \mu)^2, \mu^2, \mu^2)} \quad (85)$$

where we performed the limit $\text{Im}d_{1,1} \rightarrow \infty$ and kept only the lowest order contribution in g_θ . Therefore, in contrast to the parity allowed case, the parity forbidden thresholds do not give zero in σ^{tot} .

The reason for this behaviour may be easily understood. In the limit of $\theta \rightarrow 0$ there should not remain any effect of resonances or thresholds in σ^{tot} for parity forbidden transitions, and σ^{tot} should be described by the lowest order result (69).

Precisely this happens: Although the resonance height at $M_{1,1}^2$ remains unchanged for $\theta \rightarrow 0$, (84), its width tends to zero, (56). This means that the resonance $M_{1,1}$ still exists but is stable against $M_{1,1} \rightarrow 2\mu$ decay for $\theta \rightarrow 0$. Actually the $M_{1,1}$ bound state is a stable particle at all for $\theta = 0$. Further, at threshold $s = (M_2 + \mu)^2$, σ^{tot} tends to the first order result (69) for $\theta \rightarrow 0$,

$$\lim_{\theta \rightarrow 0} \left(\frac{4g_\theta g_\theta^*}{g_\theta + g_\theta^*} \right)^2 = m^2 \Sigma^2 + o(m^3) \quad (86)$$

as it should hold.

Remark: perhaps you would prefer a δ -function like behaviour for the stable particle limit, $\lim_{\theta \rightarrow 0} \sigma^{\text{tot}}(M_{1,1}^2) = \infty$, instead of a constant. Precisely this behaviour is present in the denominator of (85). It behaves like $\text{Im} \frac{1}{c_{1,1}(s - M_{1,1}^2) - i\epsilon_\theta \text{Im}d_2(s)}$, $\lim_{\theta \rightarrow 0} \epsilon_\theta = 0$, and, therefore, leads to the $\delta(s - M_{1,1}^2)$ behaviour for $\theta \rightarrow 0$. However, the whole transition (85) is forbidden for $\theta = 0$. Therefore, the numerator (residue of the propagator), leads to another zero for $\theta = 0$. The two limits match in a way that leads to a finite result at $s = M_{1,1}^2$, $\text{Im} \frac{\epsilon_\theta}{c_{1,1}(s - M_{1,1}^2) - i\epsilon_\theta \text{Im}d_2(s)}$. This further shows that the resonance approximation does not give any contribution at $s \neq M_{1,1}^2$ for $\theta = 0$, and, therefore, the lowest order approximation is the proper one in this case.

For even higher s , when both parity allowed and parity forbidden final states are possible, we again have the problem that the relative sign of the parity forbidden process is "wrong" due to our conventions (see the remark after equ. (55)). E.g. at the M_3 resonance we find from (81)

$$\begin{aligned} \sigma_{2\mu \rightarrow f}^{\text{tot}}(s = M_3^2) &\simeq \frac{r_1^2}{w(M_3^2, \mu^2, \mu^2)} \cdot \\ &\text{Im} \frac{g_\theta + g_\theta^* - 4g_\theta g_\theta^* \text{Red}_3(M_3^2)}{-i(g_\theta + g_\theta^*)(\text{Im}d_2(M_3^2) + \text{Im}d_{1,1}(M_3^2)) + 4ig_\theta g_\theta^* \text{Red}_3(M_3^2) \text{Im}d_2(M_3^2)} \\ &= \frac{r_1^2}{w(M_3^2, \mu^2, \mu^2)} \frac{g_\theta + g_\theta^* - \frac{4g_\theta g_\theta^*}{g_\theta + g_\theta^*}}{(g_\theta + g_\theta^* - \frac{4g_\theta g_\theta^*}{g_\theta + g_\theta^*}) \text{Im}d_2(M_3^2) + (g_\theta + g_\theta^*) \text{Im}d_{1,1}(M_3^2)} \\ &\simeq \frac{r_1^2}{w(M_3^2, \mu^2, \mu^2)} \frac{m\Sigma(\cos\theta - \frac{1}{\cos\theta})}{m\Sigma(\cos\theta - \frac{1}{\cos\theta}) \text{Im}d_2(M_3^2) + m\Sigma \cos\theta \text{Im}d_{1,1}(M_3^2)} \\ &\rightarrow \frac{r_1^2}{w(M_3^2, \mu^2, \mu^2)} \frac{\frac{1}{\cos\theta} - \cos\theta}{(\frac{1}{\cos\theta} - \cos\theta) \text{Im}d_2(M_3^2) + \cos\theta \text{Im}d_{1,1}(M_3^2)} \\ &= \frac{r_1^2}{w(M_3^2, \mu^2, \mu^2)} \frac{\sin^2\theta(\sin^2\theta \text{Im}d_2(M_3^2) + \cos^2\theta \text{Im}d_{1,1}(M_3^2))}{[\sin^2\theta \text{Im}d_2(M_3^2) + \cos^2\theta \text{Im}d_{1,1}(M_3^2)]^2} \quad (87) \end{aligned}$$

where the last two lines are for real θ (the last line may be easily checked by a low order reasoning, in case somebody does not trust our imaginary θ convention).

Again, the resonance height (containing two partial decay channels) does not depend on the coupling constant.

For even higher s the above pattern repeats.

The last thing to be discussed is the contribution of the t and u channel diagrams. There the lowest order diagram must be subtracted (see Fig. 8),

$$\mathcal{M}'_{2\mu \rightarrow 2\mu}(t) = S^T \mathcal{G}(\Pi(t) - \mathbf{1})S \quad (88)$$

where $t = 4\mu^2 - s \leq 0$, $u \equiv 0$.

It is a wellknown fact that the t and u channel amplitudes in the case at hand have no singularities on the physical sheet of the complex s plane, and, therefore, no imaginary parts (see e.g. [37]). They are, themselves, imaginary parts of some higher order graphs (in fact, of the non-factorizable four-point function of Fig. 8). As a consequence, the $\mathcal{M}'(t)$, $\mathcal{M}'(u=0)$ contributions are small for all t and cannot change the above-discussed behaviour. The only point where $\mathcal{M}'(t)$, $\mathcal{M}'(u)$ cause a qualitative change is the elastic threshold $s = 4\mu^2$, $t = 0$. There the lowest order singular behaviour, equ (69), that was cancelled by the s -channel contribution, equ. (83), is retained, but with a different coefficient. We find indeed

$$\begin{aligned} \sigma_{2\mu \rightarrow 2\mu}(s \sim 4\mu^2) &= \frac{r_1^4}{w^2(s \sim 4\mu^2, \mu^2, \mu^2)} |\mathcal{M}_{2\mu \rightarrow 2\mu}(s \sim 4\mu^2) + 2\mathcal{M}'_{2\mu \rightarrow 2\mu}(0)|^2 \\ &\simeq \frac{r_1^4}{w^2(s \sim 4\mu^2, \mu^2, \mu^2)} |2\mathcal{M}'_{2\mu \rightarrow 2\mu}(0)|^2 \\ &\simeq \frac{r_1^4}{w^2(s \sim 4\mu^2, \mu^2, \mu^2)} 4 \left(\frac{2g_\theta g_\theta^* \tilde{E}_-(0) + (g_\theta^2 + g_\theta^{*2}) \tilde{E}_+(0)}{1 - (g_\theta + g_\theta^*) \tilde{E}_+(0)} \right)^2 \\ &\rightarrow \infty \quad \text{for} \quad s \rightarrow 4\mu^2 \end{aligned} \quad (89)$$

where $\mathcal{M}_{2\mu \rightarrow 2\mu}(4\mu^2)$ is given by (71) (including the lowest order), and $\mathcal{M}'_{2\mu \rightarrow 2\mu}(0)$ is given by (88) (without lowest order). The $\tilde{E}_\pm(0)$ are just finite numbers (they have been computed in [21]).

Further, whenever the s -channel cross section vanishes (at parity allowed higher production thresholds), its value is changed from zero to a small nonzero number (of order $(m\Sigma)^4$).

All the other features of the s -channel scattering cross section remain unchanged.

VIII. SUMMARY

We have found the following features of the model in the course of our discussion:

1. The Feynman rules of mass perturbation theory acquire a matrix structure due to the chiral properties of the model (i.e. due to the fact that the mass term mixes left and right components of fields).
2. Via the Dyson-Schwinger equations of the model all the bosonic n -point functions may be re-expressed in terms of chiral (scalar and pseudoscalar) n -point functions. Further, these chiral n -point functions may be re-expressed in terms of non-factorizable ones. These non-factorizable n -point functions are the analogs of the 1PI Green functions in other theories.

3. For the two-point function this re-expression enabled us to do an exact resummation of the two-point function $\Pi(s)$ (see (19)). This resummation made it possible to identify and compute all mass poles of the stable and instable bound states of the theory, and to find all decay channels and compute all decay widths for the latter ones.
4. The same re-expression for higher n -point functions enabled us to identify all the possible initial and final states of scattering processes, and to compute these processes, where the effects of resonances and higher particle production thresholds are taken into account properly, without further assumptions or approximations.

As a result, the following physical picture emerged:

The model contains two stable particles, namely the Schwinger boson with mass μ and the two-boson bound state with mass M_2 . Further, there exist (unstable) bound states that are composed of an arbitrary number of Schwinger bosons and M_2 particles. These bound states may decay into all combinations of μ and M_2 that are possible kinematically. Those bound states that are composed of some M_2 as well are outside the common knowledge about the massive Schwinger model, but their existence is enforced by unitarity (by the way, it is not so surprising, because attractive potentials in $d = 1 + 1$ always create at least one bound state).

For scattering processes we found that far from all resonances and particle production thresholds the scattering cross section is well described by a lowest order computation (e.g. the elastic two-particle scattering cross section behaves like $\frac{1}{s^2}$ for sufficiently large s). Whenever s is near a bound state, $\sigma(s)$ has a local maximum, i.e. a resonance occurs. Moreover, for all values of s where a new final state becomes possible kinematically, the corresponding real particle production threshold indeed occurs.

All these features are results of the computations, without any further approximation in addition to the resummed mass perturbation theory.

IX. ACKNOWLEDGEMENT

The author thanks R. Jackiw for the opportunity to join the Center of Theoretical Physics at MIT, where this work was performed, and the CTP members for their hospitality. Further thanks are due to J. Pawlowski and A. Wipf for helpful discussions.

This work is supported by a Schrödinger stipendium of the Austrian FWF.

REFERENCES

- [1] J. Schwinger, Phys. Rev. *128* (1962) 2425
- [2] J. Lowenstein, J. Swieca, Ann. Phys. *68* (1971) 172
- [3] C. Jayewardena, Helv. Phys. Acta *61* (1988) 636
- [4] I. Sachs, A. Wipf, Helv. Phys. Acta *65* (1992) 653
- [5] W. Dittrich, M. Reuter, "Selected topics ...", Lecture Notes in Physics Vol. 244, Springer, Berlin 1986
- [6] Y. Frishman, Lecture Notes in Physics 32, Springer Verlag 1975
- [7] H. Grosse, "Models in statistical physics and quantum field theory", Springer, Berlin 1988
- [8] E. Abdalla, M. Abdalla, K. D. Rothe, "2 dimensional Quantum Field Theory", World Scientific, Singapore, 1991
- [9] R. Jackiw, "Topological investigations ...", in: Treiman et al, "Current algebras and anomalies", World Scientific, Singapore 1985
- [10] R. A. Bertlmann, "Anomalies in quantum field theory", Clarendon Press, Oxford 1996
- [11] N. P. Ilieva, V. N. Pervushin, Sov. J. Part. Nucl. *22* (1991) 275
- [12] C. Adam, R. A. Bertlmann, P. Hofer, Riv. Nuovo Cim. *16*, No 8 (1993)
- [13] C. Adam, Z. Phys. *C63* (1994) 169
- [14] A. Casher, J. Kogut, P. Susskind, Phys. Rev. *D10* (1974) 732
- [15] J. Kogut, P. Susskind, Phys. Rev. *D11* (1975) 3594
- [16] S. Coleman, R. Jackiw, L. Susskind, Ann. Phys. *93* (1975) 267
- [17] S. Coleman, Ann. Phys. *101* (1976) 239
- [18] J. Fröhlich, Comm. Math. Phys. *47* (1976) 233
- [19] J. Fröhlich, E. Seiler, Helv. Phys. Acta *49* (1976) 889
- [20] M. P. Fry, Phys. Rev. *D47* (1993) 2629
- [21] C. Adam, Phys. Lett. *B 363* (1995) 79, hep-ph 9507279
- [22] C. Adam, Phys. Lett. *B 382* (1996) 383, hep-ph 9507331
- [23] A. V. Smilga, Phys. Lett. *B278* (1992) 371
- [24] A. V. Smilga, Phys. Rev. *D46* (1992) 5598
- [25] A. V. Smilga, Phys. Rev. *D49* (1994) 5480
- [26] D. J. Gross, I. R. Klebanov, A. V. Matytsin, A. V. Smilga, Nucl. Phys. *B461* (1996) 109, hep-th 9511104
- [27] E. Abdalla, R. Mohayaee, A. Zadra, hep-th 9604063
- [28] C. Adam, preprint FSUJ-TPI-13/96, hep-th 9609155
- [29] M. Soldate, Ann. Phys. *158* (1984) 433
- [30] V. A. Novikov, M. A. Shifman, A. I. Vainshtein, V. I. Zakharov, Nucl. Phys. *B249* (1985) 445
- [31] C. Adam, preprint PM 96/01; hep-ph 9601227
- [32] C. Adam, Phys. Lett. *B 382* (1996) 111
- [33] J. Steele, A. Subramanian, I. Zahed, Nucl. Phys. *B452* (1995) 545, hep-th 9503220
- [34] C. Gattringer, hep-th 9503137; Ann. Phys. *250* (1996) 389, hep-th 9602027
- [35] C. Adam, preprint FSUJ-TPI-12/96, hep-th 9609154
- [36] C. Adam, preprint FSUJ-TPI-16/96, hep-th 9610050
- [37] R. J. Eden, P. V. Landshoff, D. I. Olive, J. C. Polkinghorne, "The Analytic S-Matrix", Cambridge University Press 1966